Metal-insulator crossover and massive Dirac fermions in electron-doped FeTe

Luis Craco,[1] Binjie Xu,[2] Minghu Fang,[2,3] and Byron Freelon[4]
[1]*Institute of Physics, Federal University of Mato Grosso, 78060-900 Cuiabá, Mato Grosso, Brazil*
[2]*Department of Physics, Zhejiang University, Hangzhou 310027, China*
[3]*Collaborative Innovation Center of Advanced Microstructure, Nanjing University, Nanjing 210093, China*
[4]*Department of Physics and Texas Center for Superconductivity, University of Houston, Houston, Texas 77204, USA*

(Received 31 October 2019; revised manuscript received 27 January 2020; accepted 17 March 2020; published 8 April 2020)

We explore the role played by electron doping in the electronic structure and transport properties of tetragonal FeTe using the local density approximation plus dynamical mean-field theory treatment. Semiconducting and metal-insulator crossover behavior observed in a paramagnetic and strained FeTe superconductor are shown to be driven by the interplay between multiorbital electron interactions and doping-induced normal-state massive Dirac fermions. The doping-dependent self-energy pole structure we derive is promising in the sense that it leads to results that explain why moderate electron band filling can generate orbital-selective Dirac valleys with strong electron mass enhancement consistent with experiments.

DOI: 10.1103/PhysRevB.101.165107

I. INTRODUCTION

Iron-based superconductors [1] and Dirac fermion systems [2] have attracted great attention in the material science and condensed matter community in recent years. While the bare p-band states of massless Dirac fermion systems are characterized by linear band dispersion near the Fermi energy (E_F) [2], Fe-superconducting materials show both metallic and band-gapped electronic states near E_F due to their multiorbital (MO) nature [1].

The experimentally observed Dirac cones in the 122 Fe pnictide $BaFe_2As_2$ [3,4] are known to be a consequence of zone folding in bands with different parities [3] in the magnetically ordered spin-density-wave (SDW) state, and they coexist with superconductivity in Ru-doped $BaFe_2As_2$ until the SDW vanishes [5]. Similar behavior was also reported for Ru-doped LaFeAsO [6] and Mn-doped $BaFe_2As_2$ [7], suggesting that the emergence of Dirac fermions in Fe pnictides is linked to SDW order. Although the long-range SDW order in FeTe is suppressed by Se substitution [8], spin fluctuations may still survive at low temperatures. So we cannot rule out the possibility that the origin of the Dirac cone state in Fe chalcogenide systems [9] is the same as that of Fe pnictides. However, the discovery of Dirac-cone-like ultrafast electrons in FeSe [10], Dirac-cone-type spin-helical surface states with s-wave superconducting gap below T_c in $FeTe_{0.55}Se_{0.45}$ [11], as well as the recent observation of topological transition in $FeTe_{1-x}Se_x/SrTiO_3(001)$ monolayers [12], provide new platforms for realizing Dirac-cone-like carries in 11 Fe superconductors. Thus, understanding the origin and the possibility of finding Dirac fermions (massive [13] or not) in Fe chalcogenide systems is important for understanding the role played by dynamical correlations and the emergence of Dirac-valley electronic structure in Fe-based superconductors. In this work we provide insights into the problem of MO electron-electron interactions in the tetragonal structural phase of the electron-doped FeTe parent compound, revealing the emergence of an orbital blocked phase [14] with selective linear spectrum and its implications for anomalous mass enhancement in the normal state of 11 Fe superconductors [15,16].

In the family of Fe-based superconductors, the 11 Fe chalcogenides are the simplest Fe-based superconductors with no blocking layers. They consist of a continuous stacking of Fe square-lattice layers separated by chalcogen (Te,Se) layers (see Fig. 1). However, in spite of its simple lattice structure [18] the 11-type compounds have attracted much interest in recent years due to intrinsic stronger electronic correlations [14,15,19,20] than Fe pnictides. With this in mind, we carried out local density approximation plus dynamical mean-field theory (LDA + DMFT) [21] calculations to explore the electronic structure reconstruction and transport properties of electron-doped FeTe. $Fe_{1+y}Te$ exhibits a bicollinear antiferromagnetic order [22] with an ordered moment of $2.0\mu_B$ to $2.25\mu_B$ [23], in contrast to most of the Fe-based superconductors which show a stripe antiferromagnetic ordered state below the Néel temperature, T_N. The bicollinear antiferromagnetic order is believed to be driven by frustrated magnetism of correlation-induced local moments [24]. Magnetic, transport, and structural properties of $Fe_{1+y}Te$ at low temperatures are sensitive to nonstoichiometric Fe at interstitial sites [25]: At low Fe excess, $Fe_{1+y}Te$ exhibits a first-order structural phase transition from the nonmagnetic tetragonal $P4/nmm$ phase to monoclinic $P2_1/m$. Band-structure calculations predicted tetragonal 11 Fe chalcogenides to be metallic [26]; however, $Fe_{1+y}Te$ shows nonmetallic behavior in resistivity above T_N [27], an indication of charge-carrier localization near E_F. Although angle-resolved photoemission spectroscopy (ARPES) studies show significant spectral weight near E_F, bad metallic behavior [28] and massive spectral weight redistribution [19] induced by strong correlation effects are also seen in ARPES data of $Fe_{1+y}Te$. Remarkable as well is the T-dependent spectral weight transfer (SWT) in optical conductivity spectra of Fe(Te,Se) systems [20,29,30], and the suppression of the

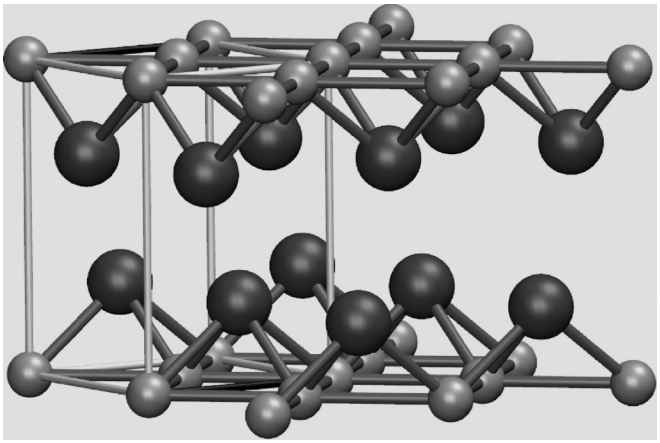

FIG. 1. Layered crystal structure of FeTe. The large and small spheres represent Te and Fe atoms, respectively. To show the arrangement of atoms, the origin of the unit cell is chosen at Fe positions [17].

Drude component at low energies due to strong electron incoherence above T_N. Taken together, the loss of low-energy spectral weight with V-shaped pseudogap features [28], the absence of Drude weight [20,29,30], and insulatinglike resistivity [29] in the nonmagnetically ordered state are fingerprints of an exotic electronic state induced by strong MO electronic interactions in FeTe [31].

The appearance of pseudogap phases [32] in strongly correlated electron systems near Mottness reveals a breakdown of the assumptions underlying the Landau-Fermi liquid theory of good metals. If the Fermi-liquid (FL) quasiparticle gives way to incoherent electronic states in exotic metals, one expects changes in the character of low-energy excitations, manifesting itself in the emergence of qualitatively new electronic behavior. In particular, these changes should manifest themselves in one- and two-particle responses [33], which probe the excitation spectrum of the non-FL state: Fe chalcogenide superconductors are particular important systems in this context, since they are among the best examples of correlated materials showing exotic normal-state properties [34]. In strained FeTe thin films [35], for example, suppression SDW order reveals superconductivity, with a transition temperature higher than that of its isostructural counterpart FeSe, and a metal-insulator crossover as in superconducting $(Tl,K,Rb)_{0.8}Fe_2Se_2$ [36]. Similar crossover behavior has also been observed in FeTe thin films at ambient pressure conditions [37] and in 25-nm FeTe flakes [38]. Thus, it is plausible to assume that suppression of SDW order by suitable external perturbations and sample preparation would reveal a semiconducting-to-bad-metal crossover with a maximum resistivity value at a characteristic and sample-dependent temperature followed by a superconducting phase transition as $T \to 0$. In this work we show that the T-dependent crossover behavior is an intrinsic normal-state property of electron-doped FeTe. Needless to say, a proper microscopic description of localization-delocalization transition [39] in 11 Fe chalcogenides is important for understanding the role played by dynamical correlations in the low-energy electronic states of Fe superconductors in general. In this work we explore the electronic structure reconstruction of electron-doped FeTe, revealing the emergence of massive Dirac fermions with predominant xz, yz orbital character due to MO electron correlation effects.

A microscopic treatment of MO electronic correlations in Fe chalcogenides is important for understanding the evolution from an orbital-blocked phase [14] to an incoherent electronic state and its implications to superconductivity [40]. Motivated thereby, in recent years systematic LDA + DMFT [21] studies were performed to understand different Fe chalcogenide systems, showing the role played by electron band filling [31] and the evolution from coherent to incoherent electronic structure [41] and its relationship to the one- and two-particle features seen in experiment. Following earlier studies [31,42], here we undertake a comprehensive LDA + DMFT study of dynamical MO electron-electron interactions in FeTe, showing how electronic localization seen in resistivity measurements [43] and the emergence of V-shaped Dirac quasiparticles [28] can be understood within a single theoretical picture. Good semiquantitative agreement with resistivity data of paramagnetic $Fe_{1.1}Te$ [43] (see inset of Fig. 3) serves as support to our proposal of correlation-induced anisotropic Dirac-like band dispersion [16] in electron-doped FeTe superconductors.

II. RESULTS AND DISCUSSION

The relevant inputs in our theory are the LDA density of states (DOS) for the five $3d$ orbitals already discussed in Ref. [31], the on-site Coulomb interaction U, the interorbital term $U' = U - 2J_H$, and the Hund coupling. With this the correlated many-body Hamiltonian for FeTe reads $H = \sum_{\mathbf{k},a,\sigma} \epsilon_{\mathbf{k},a} c^{\dagger}_{\mathbf{k},a,\sigma} c_{\mathbf{k},a,\sigma} + U \sum_{i,a} n_{ia\uparrow} n_{ia\downarrow} U' \sum_{i,a\neq b} n_{ia} n_{ib} - J_H \sum_{i,a\neq b} \mathbf{S}_{ia} \cdot \mathbf{S}_{ib}$. Here, $a = (x^2 - y^2, 3z^2 - r^2, xz, yz, xy)$ denotes the diagonalized $3d$ orbitals of FeTe. We evaluate the many-particle Green's functions of the Hamiltonian above within LDA + DMFT [21], using MO iterated perturbation theory (MO-IPT) as an impurity solver [44].

In order to address the emergence of orbital-selective Dirac fermions in the nonmagnetically ordered state of electron-doped FeTe, below we present LDA + DMFT results for fixed values of $U = 4\,\text{eV}$ and $J_H = 0.7\,\text{eV}$. Here we follow Ref. [14], which also employed fixed Coulomb interaction parameters to study a series of Fe-based materials, showing that changes in their physical properties are mainly due to variations in the one-band structural inputs and small differences in the total electron occupation (n) of the iron $3d$ shell, rather than changes in the screening of the MO Coulomb interactions [45] or by the mutual interplay between U, U', and J_H [46].

To begin with, in Fig. 2 we display the effect of MO electron-electron interactions on the orbital-resolved spectral functions of tetragonal FeTe. As seen, the LDA + DMFT spectral functions are highly reshaped by electron-electron interactions compared to LDA [47]. Similar to FeSe [41], at $U = 4.0\,\text{eV}$ (and $J_H = 0.7\,\text{eV}$), FeTe is a non-FL metal with an orbital-dependent pseudoband gap and lower Hubbard bands (LHBs) centered at energies close to 4.0 eV binding energy on all orbitals. As seen, the $3z^2 - r^2, x^2 - y^2, xy$ orbitals show stronger correlation effects with pronounced

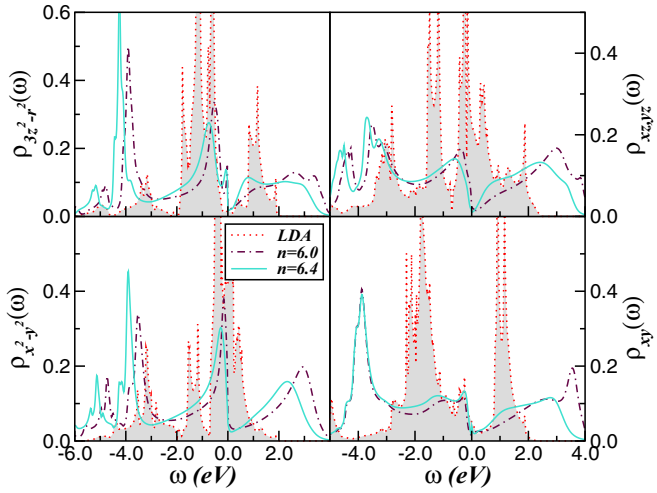

FIG. 2. Orbital-resolved LDA and LDA + DMFT (with $U = 4.0\,\text{eV}$, $U' = 2.6\,\text{eV}$, and $J_H = 0.7\,\text{eV}$) density of states (DOS) for the Fe $3d$ orbitals of tetragonal FeTe [31]. An important feature to be seen in the LDA results is the fact that all d bands span over the Fermi level, $E_F = \omega = 0$. This confirms that the electronic states relevant to FeTe are Fe $3d$ states. Noteworthy is the electronic reconstruction with increasing the total electron concentration of the Fe $3d$ shell. Here, all LDA + DMFT spectral functions are computed at zero temperature.

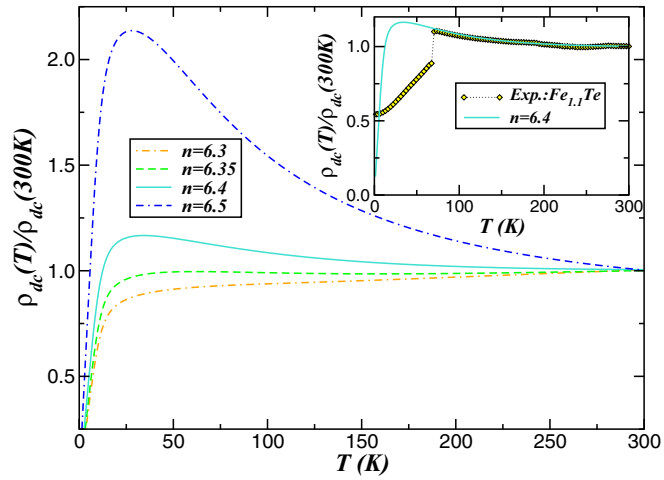

FIG. 3. Resistivity versus temperature (normalized at 300 K) of electron-doped FeTe, showing the evolution from a saturated high-T metal to a semiconducting-like system with increasing total electron concentration n of the Fe $3d$ shell. An important feature to be seen is the appearance of low-T metal-to-insulator crossover at $n = 6.35$. The inset displays our resistivity data for $Fe_{1.1}Te$ [43]: Good agreement with experiment in the paramagnetic state above $T_N = 70\,\text{K}$ is obtained for $n = 6.4$.

LHBs while the xz, yz orbitals display less tendency towards local moment formation (LHB). Additionally, upon electron doping the parent FeTe compound, the LDA + DMFT orbital-resolved spectral function shows large-scale changes in SWT with increasing the total band filling n of the Fe $3d$ shell. As seen in Fig. 2, the LDA + DMFT treatment [31] for tetragonal FeTe introduces nontrivial effects stemming from the dynamical nature of sizable local electronic correlations. As shown here, these MO scattering processes lead to large SWT across large energy scales in response to small changes in the total band filling (see our results below), a characteristic lying at the heart of the anomalous responses of strongly correlated electron systems close to Mottness.

To make contact with experiment in Fig. 3 we show the effect of electron doping $n = 6.0 + \delta$ on the dc resistivity of the FeTe parent compound. One striking feature of our results for $n = 6.3$ is the saturating resistivity from 50 K up to room temperature. Similar behavior has been observed in superconducting $FeTe_{1-x}Se_x$ single and polycrystals [34,48,49] and films [50] as well as in strained FeTe superconductors [35], suggesting a similar incoherent normal state above a characteristic, sample-dependent temperature. Moreover, focusing on the metal-insulator crossover as a result of softening the first-order SDW phase transition [35], we make contact with our experimental data for $Fe_{1.1}Te$. [43] Similar resistivity T dependence was also obtained by other groups [20,29,51], suggesting a common underlying low-energy scenario for $Fe_{1+y}Te$.

As seen in the inset of Fig. 3, LDA + DMFT (MO-IPT) provides a compelling description of observed experimental data above T_N, supporting the view of strong electronic correlations in 11 Fe chalcogenides [16]. It is noteworthy that in an earlier study [31] the origin of the insulatinglike form (above $T_N \approx 65\,\text{K}$) seen in $Fe_{1.1}Te$ has been clarified microscopically [43]. It was shown there that orbital-selective incoherence characterizes the paramagnetic phase in layered Fe(Se,Te) systems in general. According to our LDA + DMFT results below the emergence of a metal-insulator crossover in paramagnetic FeTe should be considered a manifestation of slightly increasing the band filling via electron doping [14] or Fe excess [34,49,52] of an orbital-selective metal in close proximity to Mott localization [53]. As seen in Fig. 3, ρ_{dc} dramatically increases between $n = 6.4$ and 6.5, implying that orbital-selective localization is promoted with increasing the carrier concentration of the Fe $3d$ shell [39].

To get realistic insights into the MO correlated electronic state and the hidden Dirac-liquid regime in electron-doped FeTe, in Fig. 4 we display its orbital-resolved DOS. Particular features to be seen are the two pronounced $x^2 - y^2$, $3z^2 - r^2$ waterfall structures [54] above the corresponding LHBs: The former implies an intrinsic electronic tendency towards local moment formation [55] in FeTe. In addition, our results reveal pseudogaplike features with strongly anisotropic and orbital-dependent V-shaped features at low energies: It is worth noting here that the existence of V-shaped DOS $\rho(\omega) \approx |\omega|$ at energies close to the neutrality Dirac point is a distinctive feature of graphene and topological insulators [2]. Particularly interesting in this context is Dirac-like electronic dispersion in the xz, yz orbital states, showing almost perfect linear falloff near E_F (see inset of Fig. 4). The absence of a true minimum value expected to be seen in noninteracting Dirac fermion gas results from the fact that Dirac quasiparticles in doped FeTe are driven by strong correlations and not by free electron bare band topology [2]. Thus, the finite background DOS observed in the inset of Fig. 4 near the correlated Dirac point is an intrinsic property of interacting Dirac fermions [56].

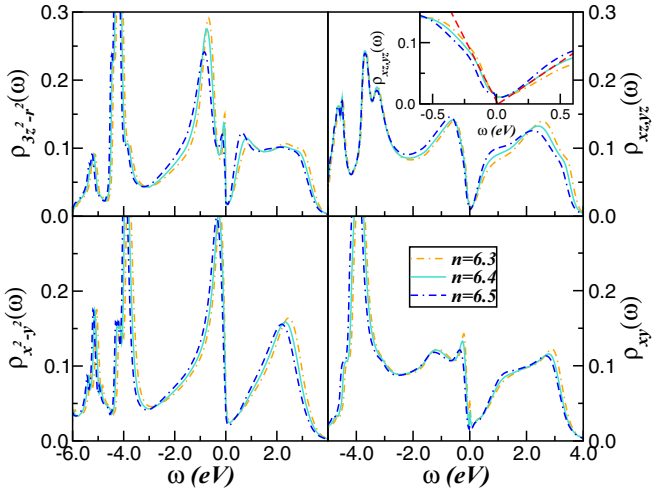

FIG. 4. Orbital-resolved LDA + DMFT (with $U = 4.0$ eV and $J_H = 0.7$ eV) DOS for the Fe $3d$ orbitals of electron-doped ($n = 6.0 + \delta$) FeTe. Notice the nearly perfect V-shaped Dirac-like DOS within the xz, yx orbitals and the correlation-induced waterfalls [54] followed by narrow lower Hubbard bands in the $3z^2 - r^2, x^2 - y^2$ orbital sector.

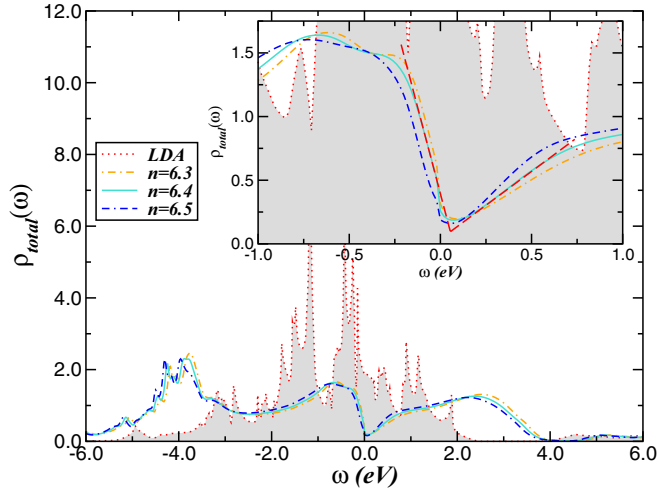

FIG. 5. Comparison between LDA [31] and LDA + DMFT (MO-IPT) total DOS of FeTe. Notice the large spectral weight transfer induced by strong electron-electron interactions in the solid. The inset shows the energy window where tetragonal FeTe exhibits an almost linear falloff DOS near E_F for $n = 6.4$.

Taken together, our results in Fig. 4 show that coexistence of pseudogapped and quasilinear spectral functions near E_F can be tuned in bulk FeTe by electron doping the parent compound. They also seem to suggest that the shape of the Dirac cones in electron-doped FeTe would be anisotropic, consistent with observations for $BaFe_2As_2$ [3] whose apex is also located slightly above E_F. This result can be taken as additional evidence that the MO Coulomb perturbation [57] is a natural way to approach Dirac fermions in tetragonal Fe chalcogenide systems [16,48]. If our proposal is to hold, the metal-insulator crossover in electron-doped FeTe should be characterized by pseudogapped electronic states and massive Dirac-like fermions with $3z^2 - r^2, xz, yx$ orbital character (see our results below). Thus, within the hidden Dirac-liquid phase the reconstructed Fermi surface is expected to be composed of two distinct MO components, and future ARPES experiments could verify this aspect.

On general grounds and relevant to scanning tunneling microscopy (STM) experiments, our main result in Fig. 5 shows that V-shaped linear dispersions with asymmetric Dirac-cone-like carriers [10] can be tuned in the total DOS of bulk FeTe by electron doping. We notice here that the experimental DOS curves probed by STM spectroscopy are never simple symmetric V-shaped curves [56]; thus, it is plausible to assume that similar valley DOS as in Fig. 5 would be seen in future tunneling experiments. Although the weight of the Dirac state is relatively broad near E_F and the contribution of the pseudogapped bands must be suppressed to extract the unique carrier transport intrinsic to Dirac cones, the mobility of lighter $x^2 - y^2, xy$ Dirac fermions would dominate electronic transport in electron-doped FeTe.

Our results in Figs. 4 and 5 clearly call for a deeper microscopic understanding of the orbital-selective V-shaped DOS and the metal-insulator crossover discussed above. In DMFT, the evolution of $\rho_{dc}(T)$ is intimately linked to self-energy corrections and the δ-dependent evolution of the spectral functions. In Fig. 6, we show the imaginary and real parts of the orbital-resolved self-energies, $[\mathrm{Im}\Sigma_a(\omega)]$ and $[\mathrm{Re}\Sigma_a(\omega)]$, respectively, computed within LDA + DMFT for $0.3 < \delta < 0.5$ in order to facilitate this link. Strong energy dependence of the LDA + DMFT self-energies is clearly seen: This provides a microscopic basis for rationalizing electron correlation effects [19] and the nature of bad metallic behavior [28] in $Fe_{1+y}Te$ and related Fe(Se,Te) systems [15,34,37,48,50]. In Fig. 6 we identify two relevant self-energy structures, the strongly incoherent V-shaped-like behavior on all orbitals and the pole generating the proximity to Mott-Dirac electronic localization in the $3z^2 - r^2, xz, yz$ orbital sector. As seen, due

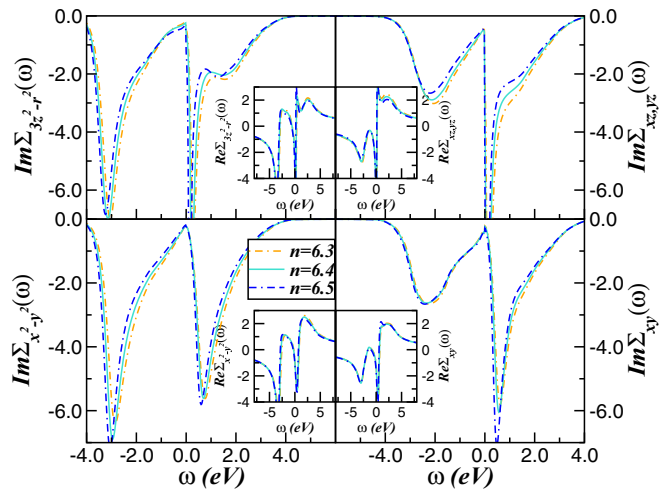

FIG. 6. Orbital-resolved (LDA + DMFT) self-energies, imaginary (main panels) and real (insets) parts, for the Fe $3d$ orbitals of electron-doped FeTe. The selective-orbital nature is clearly visible. Notice the sharp poles in imaginary parts of the self-energies near E_F for the strongly correlated $3z^2 - r^2, xz, yz$ orbital sector.

to interplay between MO electron-electron interactions and doping-dependent SWT, the pole structure evolves continuously towards E_F into the hidden orbital-selective insulating state of $Fe_{1+y}Te$. Thus, at low T we find that $\rho_{dc}(T) \simeq T$ correlates with an orbital-selective incoherent spectral function found in earlier LDA + DMFT works [16,41] where $\mathrm{Im}\Sigma(\omega) \simeq -|\omega|$ at low energy, while at higher T the pole structure in the $3z^2 - r^2, xz, yz$ orbitals at $n = 6.4$ and 6.5 is responsible for the semiconducting behavior as displayed in Fig. 3. We predict that similar features as in Fig. 6 would be seen in scattering rates $\tau^{-1}(\omega) \simeq \Im\Sigma(\omega)$ [58], and future ARPES or optical conductivity studies are called for to confirm our prediction. Finally, since in DMFT the self-energy is momentum independent, the quasiparticle residue Z_a of an orbital a, which defines the renormalized Fermi energy, directly yields the effective electron mass enhancement: $\frac{m_a^\star}{m_e} = \frac{1}{Z_a} = (1 - \frac{\partial \mathrm{Re}\Sigma_a(\omega)}{\partial\omega})_{\omega=0}$, where m_e is the free electron mass. Thus, from the slope of the self-energy real part in Fig. 6 we obtain for $n = 6.4$ $(\frac{m^\star_{3z^2-r^2}}{m_e}, \frac{m^\star_{xz,yz}}{m_e}, \frac{m^\star_{x^2-y^2}}{m_e}, \frac{m^\star_{xy}}{m_e}) = (15.9, 25.6, 6.6, 4.5)$ in good qualitative accord with values $\frac{m^\star}{m_e} \approx$ 6–20 found in ARPES for $FeSe_{0.42}Te_{0.58}$ [15], attesting to the strong electron correlation effects in the normal state of 11 Fe chalcogenides.

It is worth noting as well that $\Sigma_a(\omega)$ renormalizes the relative band positions depending upon their orbital occupations. As a consequence of Mott-Diracness, the two-fluid metal (comprised of a pseudogapped Dirac-like spectrum) found in FeTe at the border of the doping-induced selective Dirac valleytronics is totally incoherent at normal conditions. Clear deviations from the ω^2 dependence of a canonical FL, with (sub)linear ω dependence of marginal Fermi liquids [59], is seen in Fig 6. Similar self-energy behavior as in Fig. 6, with sublinear energy dependencies, was also found in earlier studies [16,60,61], suggesting a common scenario of correlation-induced electronic reconstruction in Fe chalcogenides. Interestingly, the departure from the FL behavior caused by many-body interactions has been also reported for quasi-freestanding graphene and Bi_2Te_2Se topological insulators [62], showing a similar marginal form as shown here.

Our results revealed important aspects for the correlated electronic structure reconstruction in $Fe_{1+y}Te$. Within LDA + DMFT we have shown that an orbital-selective Dirac-like spectrum in the bulk arises from strong electron-electron interactions and the proximity to Mott localization as in FeS superconductors [16]. For an electron band filling of $n = 6.4$ the xz, yz orbital sector of FeTe exhibits an almost perfect linear falloff of the electronic spectrum near E_F and large mass enhancement, a characteristic akin to strongly correlated Dirac fermions [63]. We thus predict that in electron-doped FeTe substantial changes would be seen when the Mott-Dirac regime is approached, including an electronic reconstruction with similarities to marginal Fermi liquids. Our results suggest a promising route for realizing the Mott-Dirac electronic state [64], where orbital-selective Dirac bands result from strong electron-electron interactions in the bulk. However, whether a topologically nontrivial Dirac semimetal, with s-wave superconducting gap below T_c [11], will be observed in $Fe_{1+y}Te$ remains to be seen in future studies. If this holds true, superconducting FeTe is expected to be a possible alternative platform to Fe(Se,Te) superconductors [9,65] for realizing Majorana zero-energy vortex bound states.

III. CONCLUSION

To summarize, we have used LDA + DMFT for a five-band Hubbard model to give a more detailed analysis of the doping evolution of the strongly correlated spectral functions and self-energies of tetragonal FeTe. The metal-insulator crossover seen in transport of Fe(Te,Se) arises from anomalous self-energy pole structures near E_F due to interplay between electron doping and many-particle correlation effects. For an electron band filling of $n = 6.4$ the xz, yz orbital sectors exhibit an almost perfect linear falloff density of states near E_F and large mass enhancement. These responses can be directly tested by a combination of spectral and transport measurements in FeTe with Fe excess. Such studies are called for, and should confirm or refute our proposal. Moreover, the interplay between Mott-Dirac localization and bad itinerancy in electron-doped FeTe suggests a promising and practical route to access electron pairing on bands without Fermi surfaces [66] and Majorana quasiparticles [9,65] via multiple Dirac-like bulk states but this remains to be seen in the future.

ACKNOWLEDGMENTS

L.C.'s work was supported by CNPq (Grant No. 304035/2017-3). B.X. and M.F. are grateful for support from the Ministry of Science and Technology of China under Grants No. 2016YFA0300402 and No. 2015CB921004 and the National Natural Science Foundation of China (NSFC) (Grant No. 11374261), and are supported by the Fundamental Research Funds for the Central Universities. B.F. was supported by the Department of Physics and the State of Texas through the Texas Center for Superconductivity at the University of Houston. Acknowledgment (L.C.) is also made to CAPES.

[1] D. C. Johnston, Adv. Phys. **59**, 803 (2010); G. R. Stewart, Rev. Mod. Phys. **83**, 1589 (2011).

[2] A. H. Castro Neto, F. Guinea, N. M. R. Peres, K. S. Novoselov, and A. K. Geim, Rev. Mod. Phys. **81**, 109 (2009); M. Z. Hasan and C. L. Kane, *ibid.* **82**, 3045 (2010).

[3] P. Richard, K. Nakayama, T. Sato, M. Neupane, Y.-M. Xu, J. H. Bowen, G. F. Chen, J. L. Luo, N. L. Wang, X. Dai, Z. Fang, H. Ding, and T. Takahashi, Phys. Rev. Lett. **104**, 137001 (2010).

[4] K. K. Huynh, Y. Tanabe, and K. Tanigaki, Phys. Rev. Lett. **106**, 217004 (2011).

[5] Y. Tanabe, K. K. Huynh, S. Heguri, G. Mu, T. Urata, J. Xu, R. Nouchi, N. Mitoma, and K. Tanigaki, Phys. Rev. B **84**, 100508(R) (2011); Y. Tanabe, K. K. Huynh, T. Urata, S. Heguri,

G. Mu, J. T. Xu, R. Nouchi, and K. Tanigaki, *ibid.* **86**, 094510 (2012).

[6] I. Pallecchi, F. Bernardini, M. Tropeano, A. Palenzona, A. Martinelli, C. Ferdeghini, M. Vignolo, S. Massidda, and M. Putti, Phys. Rev. B **84**, 134524 (2011).

[7] T. Urata, Y. Tanabe, K. K. Huynh, H. Oguro, K. Watanabe, S. Heguri, and K. Tanigaki, Phys. Rev. B **89**, 024503 (2014).

[8] T. J. Liu, J. Hu, B. Qian, D. Fobes, Z. Q. Mao, W. Bao, M. Reehuis, S. A. J. Kimber, K. Proke, S. Matas, D. N. Argyriou, A. Hiess, A. Rotaru, H. Pham, L. Spinu, Y. Qiu, V. Thampy, A. T. Savici, J. A. Rodriguez, and C. Broholm, Nat. Mater. **9**, 718 (2010).

[9] P. Zhang, Z. Wang, X. Wu, K. Yaji, Y. Ishida, Y. Kohama, G. Dai, Y. Sun, C. Bareille, K. Kuroda, T. Kondo, K. Okazaki, K. Kindo, X. Wang, C. Jin, J. Hu, R. Thomale, K. Sumida, S. Wu, K. Miyamoto, T. Okuda, H. Ding, G. D. Gu, T. Tamegai, T. Kawakami, M. Sato, and S. Shin, Nat. Phys. **15**, 41 (2019).

[10] K. K. Huynh, Y. Tanabe, T. Urata, H. Oguro, S. Heguri, K. Watanabe, and K. Tanigaki, Phys. Rev. B **90**, 144516 (2014).

[11] P. Zhang, K. Yaji, T. Hashimoto, Y. Ota, T. Kondo, K. Okazaki, Z. Wang, J. Wen, G. D. Gu, H. Ding, and S. Shin, Science **360**, 182 (2018); see also J. D. Rameau, N. Zaki, G. D. Gu, P. D. Johnson, and M. Weinert, Phys. Rev. B **99**, 205117 (2019).

[12] X.-L. Peng, Y. Li, X.-X. Wu, H.-B. Deng, X. Shi, W.-H. Fan, M. Li, Y.-B. Huang, T. Qian, P. Richard, J.-P. Hu, S.-H. Pan, H.-Q. Mao, Y.-J. Sun, and H. Ding, Phys. Rev. B **100**, 155134 (2019).

[13] K. S. Kim, A. L. Walter, L. Moreschini, T. Seyller, K. Horn, E. Rotenberg, and A. Bostwick, Nat. Mater. **12**, 887 (2013); see also B. A. Assaf, T. Phuphachong, V. V. Volobuev, A. Inhofer, G. Bauer, G. Springholz, L. A. de Vaulchier, and Y. Guldner, Sci. Rep. **6**, 20323 (2016).

[14] Z. P. Yin, K. Haule, and G. Kotliar, Nat. Mater. **10**, 932 (2011).

[15] A. Tamai, A. Y. Ganin, E. Rozbicki, J. Bacsa, W. Meevasana, P. D. C. King, M. Caffio, R. Schaub, S. Margadonna, K. Prassides, M. J. Rosseinsky, and F. Baumberger, Phys. Rev. Lett. **104**, 097002 (2010).

[16] L. Craco and S. Leoni, Sci. Rep. **7**, 46439 (2017).

[17] L. Craco and S. Leoni, Europhys. Lett. **92**, 67003 (2010).

[18] A. Martinelli, A. Palenzona, M. Tropeano, C. Ferdeghini, M. Putti, M. R. Cimberle, T. D. Nguyen, M. Affronte, and C. Ritter, Phys. Rev. B **81**, 094115 (2010).

[19] Y. Zhang, F. Chen, C. He, L. X. Yang, B. P. Xie, Y. L. Xie, X. H. Chen, M. Fang, M. Arita, K. Shimada, H. Namatame, M. Taniguchi, J. P. Hu, and D. L. Feng, Phys. Rev. B **82**, 165113 (2010).

[20] Y. M. Dai, A. Akrap, J. Schneeloch, R. D. Zhong, T. S. Liu, G. D. Gu, Q. Li, and C. C. Home, Phys. Rev. B **90**, 121114(R) (2014).

[21] G. Kotliar, S. Y. Savrasov, K. Haule, V. S. Oudovenko, O. Parcollet, and C. A. Marianetti, Rev. Mod. Phys. **78**, 865 (2006).

[22] D. W. Tam, H.-H. Lai, J. Hu, X. Lu, H. C. Walker, D. L. Abernathy, J. L. Niedziela, T. Weber, M. Enderle, Y. Su, Z. Q. Mao, Q. Si, and P. Dai, Phys. Rev. B **100**, 054405 (2019).

[23] S. Li, C. de la Cruz, Q. Huang, Y. Chen, J. W. Lynn, J. Hu, Y.-L. Huang, F.-C. Hsu, K.-W. Yeh, M.-K. Wu, and P. Dai, Phys. Rev. B **79**, 054503 (2009); W. Bao, Y. Qiu, Q. Huang, M. A. Green, P. Zajdel, M. R. Fitzsimmons, M. Zhernenkov, S. Chang, M. Fang, B. Qian, E. K. Vehstedt, J. Yang, H. M. Pham, L. Spinu, and Z. Q. Mao, Phys. Rev. Lett. **102**, 247001 (2009).

[24] H.-H. Lai, S.-S. Gong, W.-J. Hu, and Q. Si, arXiv:1608.08206.

[25] D. Fobes, I. A. Zaliznyak, Z. Xu, R. Zhong, G. Gu, J. M. Tranquada, L. Harriger, D. Singh, V. O. Garlea, M. Lumsden, and B. Winn, Phys. Rev. Lett. **112**, 187202 (2014) and references therein.

[26] A. Subedi, L. Zhang, D. J. Singh, and M. H. Du, Phys. Rev. B **78**, 134514 (2008).

[27] M. H. Fang, H. M. Pham, B. Qian, T. J. Liu, E. K. Vehstedt, Y. Liu, L. Spinu, and Z. Q. Mao, Phys. Rev. B **78**, 224503 (2008).

[28] P. H. Lin, Y. Texier, A. Taleb-Ibrahimi, P. Le Fevre, F. Bertran, E. Giannini, M. Grioni, and V. Brouet, Phys. Rev. Lett. **111**, 217002 (2013).

[29] G. F. Chen, Z. G. Chen, J. Dong, W. Z. Hu, G. Li, X. D. Zhang, P. Zheng, J. L. Luo, and N. L. Wang, Phys. Rev. B **79**, 140509(R) (2009).

[30] C. Mirri, P. Calvani, F. M. Vitucci, A. Perucchi, K. W. Yeh, M. K. Wu, and S. Lupi, Supercond. Sci. Technol. **25**, 045002 (2012).

[31] L. Craco and S. Leoni, Mater. Res. Express **1**, 036001 (2014).

[32] I. Pallecchi, M. Tropeano, C. Ferdeghini, G. Lamura, A. Martinelli, A. Palenzona, and M. Putti, J. Supercond. Nov. Magn. **24**, 1751 (2011).

[33] M. Klein, A. Nuber, F. Reinert, J. Kroha, O. Stockert, and H. v. Löhneysen, Phys. Rev. Lett. **101**, 266404 (2008); N. Doiron-Leyraud, I. R. Walker, L. Taillefer, M. J. Steiner, S. R. Julian, and G. G. Lonzarich, Nature (London) **425**, 595 (2003).

[34] C. Dong, H. Wang, Z. Li, J. Chen, H. Q. Yuan, and M. Fang, Phys. Rev. B **84**, 224506 (2011).

[35] Y. Han, W. Y. Li, L. X. Cao, X. Y. Wang, B. Xu, B. R. Zhao, Y. Q. Guo, and J. L. Yang, Phys. Rev. Lett. **104**, 017003 (2010).

[36] M.-H. Fang, H.-D. Wang, C.-H. Dong, Z.-J. Li, C.-M. Feng, J. Chen, and H. Q. Yuan, Europhys. Lett. **94**, 27009 (2011); Y. Zhou, D.-H. Xu, F.-C. Zhang, and W.-Q. Chen, *ibid.* **95**, 17003 (2011).

[37] I. Tsukada, M. Hanawa, S. Komiya, A. Ichinose, T. Akiike, Y. Imai, and A. Maeda, Physica C **471**, 625 (2011).

[38] T.-W. Hsieh, T. Zhou, J. Hu. Z. Q. Mao, P. P. Zhang, and X. Ke, J. Phys.: Condens. Matter **30**, 295303 (2018).

[39] L. Craco, M. S. Laad, and S. Leoni, Europhys. Lett. **91**, 27001 (2010).

[40] T. Hanaguri, S. Niitaka, K. Kuroki, and H. Takagi, Science **328**, 474 (2010); E. Ieki, K. Nakayama, Y. Miyata, T. Sato, H. Miao, N. Xu, X.-P. Wang, P. Zhang, T. Qian, P. Richard, Z.-J. Xu, J. S. Wen, G. D. Gu, H. Q. Luo, H.-H. Wen, H. Ding, and T. Takahashi, Phys. Rev. B **89**, 140506(R) (2014).

[41] L. Craco, M. S. Laad, and S. Leoni, J. Phys.: Conf. Ser. **487**, 012017 (2014).

[42] L. Craco, Solid State Commun. **253**, 14 (2017).

[43] We grew the $Fe_{1.1}Te$ crystals by using a self-flux method. Then the single crystals as grown were annealed in air at 270°C for 3 h to remove some excess Fe atoms, and the crystals of $Fe_{1.1}Te$ were obtained, in which the Fe amount was determined by the energy-dispersive x-ray (EDXS) method, as reported in Ref. [34]. The resistance was measured using the standard four-probe method with a Quantum Design Physical Property Measurement System (PPMS-9).

[44] L. Craco, Phys. Rev. B **77**, 125122 (2008).
[45] M. Hirayama, T. Miyake, and M. Imada, Phys. Rev. B **87**, 195144 (2013).
[46] N. Lanatà, H. U. R. Strand, G. Giovannetti, B. Hellsing, L. de' Medici, and M. Capone, Phys. Rev. B **87**, 045122 (2013).
[47] Within the tetragonal lattice structure [18], one-electron band-structure calculations based on LDA were performed in a previous study (see Ref. [31] and references therein) for FeTe using the linear muffin-tin orbitals scheme in the atomic sphere approximation.
[48] Y. Sun, T. Taen, T. Yamada, S. Pyon, T. Nishizaki, Z. Shi, and T. Tamegai, Phys. Rev. B **89**, 144512 (2014).
[49] K. Deguchi, A. Yamashita, T. Yamaki, H. Hara, S. Demura, S. J. Denholme, M. Fujioka, H. Okasaki, H. Takeya, T. Yamaguchi, and Y. Takano, J. Appl. Phys. **115**, 053909 (2014).
[50] H. H. Chang, J. Y. Luo, C. T. Wu, F. C. Hsu, T. W. Huang, P. M. Wu, M. K. Wu, and M. J. Wang, Supercond. Sci. Technol. **25**, 035004 (2012).
[51] T. J. Liu, X. Ke, B. Qian, J. Hu, D. Fobes, E. K. Vehstedt, H. Pham, J. H. Yang, M. H. Fang, L. Spinu, P. Schiffer, Y. Liu, and Z. Q. Mao, Phys. Rev. B **80**, 174509 (2009); T. Gebre, G. Li, J. B. Whalen, B. S. Conner, H. D. Zhou, G. Grissonnanche, M. K. Kostov, A. Gurevich, T. Siegrist, and L. Balicas, *ibid.* **84**, 174517 (2011); E. E. Rodriguez, D. A. Sokolov, C. Stock, M. A. Green, O. Sobolev, J. A. Rodriguez-Rivera, H. Cao, and A. Daoud-Aladine, *ibid.* **88**, 165110 (2013).
[52] A. M. Turner, F. Wang, and A. Vishwanath, Phys. Rev. B **80**, 224504 (2009).
[53] G. Baskaran, J. Phys. Soc. Jpn. **77**, 113713 (2008); S. Pankov and V. Dobrosavljević, Phys. Rev. B **77**, 085104 (2008).
[54] S. Sakai, M. Civelli, and M. Imada, Phys. Rev. B **98**, 195109 (2018) and references therein.
[55] A. Liebsch and H. Ishida, Phys. Rev. B **82**, 155106 (2010).
[56] A. Principi, M. Polini, R. Asgari, and A. H. MacDonald, Solid State Commun. **152**, 1456 (2012).
[57] L. A. Wray, S.-Y. Xu, Y. Xia, D. Hsieh, A. V. Fedorov, Y. S. Hor, R. J. Cava, A. Bansil, H. Lin, and M. Z. Hasan, Nat. Phys. **7**, 32 (2011).
[58] J. Fink, J. Nayak, E. D. L. Rienks, J. Bannies, S. Wurmehl, S. Aswartham, I. Morozov, R. Kappenberger, M. A. ElGhazali, L. Craco, H. Rosner, C. Felser, and B. Büchner, Phys. Rev. B **99**, 245156 (2019).
[59] C. M. Varma, P. B. Littlewood, S. Schmitt-Rink, E. Abrahams, and A. E. Ruckenstein, Phys. Rev. Lett. **63**, 1996 (1989).
[60] L. Craco, M. S. Laad, and S. Leoni, Phys. Rev. B **84**, 224520 (2011).
[61] B. Freelon, Y. Hao Liu, J.-L. Chen, L. Craco, M. S. Laad, S. Leoni, J. Chen, L. Tao, H. Wang, R. Flauca, Z. Yamani, M. Fang, C. Chang, J.-H. Guo, and Z. Hussain, Phys. Rev. B **92**, 155139 (2015).
[62] D. A. Siegel, C.-H. Park, C. Hwang, J. Deslippe, A. V. Fedorov, S. G. Louie, and A. Lanzara, Proc. Natl. Acad. Sci. USA **108**, 11365 (2011); L. Craco and S. Leoni, Phys. Rev. B **85**, 195124 (2012).
[63] H. Pirie, Y. Liu, A. Soumyanarayanan, P. Chen, Y. He, M. M. Yee, P. F. S. Rosa, J. D. Thompson, D.-J. Kim, Z. Fisk, X. Wang, J. Paglione, D. K. Morr, M. H. Hamidian, and J. E. Hoffman, Nat. Phys. **16**, 52 (2020).
[64] H. L. Feng, S. Calder, M. P. Ghimire, Y.-H. Yuan, Y. Shirako, Y. Tsujimoto, Y. Matsushita, Z. Hu, C.-Y. Kuo, L. H. Tjeng, T.-W. Pi, Y.-L. Soo, J. He, M. Tanaka, Y. Katsuya, M. Richter, and K. Yamaura, Phys. Rev. B **94**, 235158 (2016).
[65] T. Machida, Y. Sun, S. Pyon, S. Takeda, Y. Kohsaka, T. Hanaguri, T. Sasagawa, and T. Tamegai, Nat. Mater. **18**, 811 (2019).
[66] H. Miao, T. Qian, X. Shi, P. Richard, T. K. Kim, M. Hoesch, L. Y. Xing, X. C. Wang, C. Q. Jin, J. P. Hu, and H. Ding, Nat. Commun. **6**, 6056 (2015).